Macromolecules

pubs.acs.org/Macromolecules Article

New Generation of Thermoplastic Elastomers from Narrowly Dispersed All-(Meth)acrylic ABA Triblock Copolymers Made by RAFT

Maksym Odnoroh, Oleksandr Ivanchenko, Guillaume Fleury, Marc Guerre,* and Mathias Destarac*

Cite This: *Macromolecules* 2024, 57, 9565−9575 Read Online

ACCESS | Metrics & More | Article Recommendations | Supporting Information

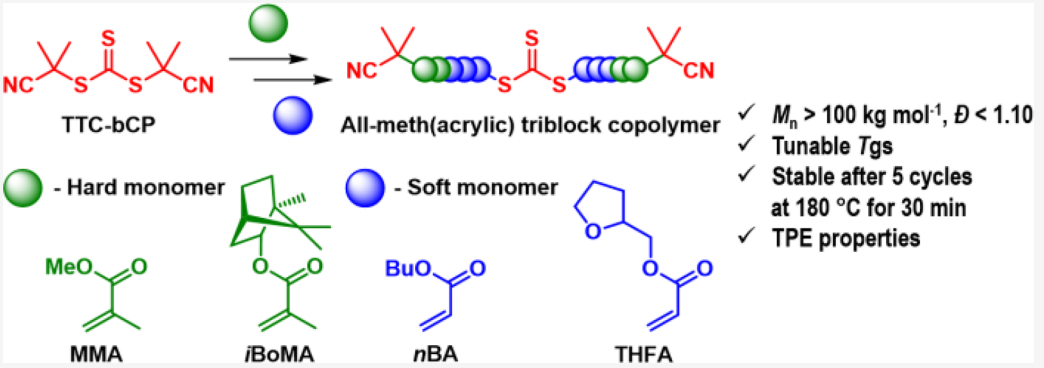

ABSTRACT: Symmetrical trithiocarbonate (TTC) bis(2-cyanopropan-2-yl)trithiocarbonate (**TTC-bCP**) was investigated in reversible addition−fragmentation chain transfer polymerization for the synthesis of a library of well-defined all-meth(acrylic) ABA triblock copolymers with thermoplastic elastomeric properties. In addition to standard monomers such as methyl methacrylate (MMA) and *n*-butyl acrylate, biobased monomers such as isobornyl methacrylate (*i*BoMA) and tetrahydrofurfuryl acrylate were used. High molar masses (>100 kg mol^{-1}) with low dispersities (<1.10) were achieved, and variation of the hard block composition between MMA and *i*BoMA allowed to tune the service temperature between 120 and 180 °C. The obtained materials have been shown to exhibit invariant storage modulus (G') in the MPa range after 5 cycles of recycling at 180 °C for 30 min

INTRODUCTION

Thermoplastic elastomers (TPEs) share the advantages of both rubbery and thermoplastic materials. Although discovered in the 1950s,[1,2] they recently gained increasing attention, as they exhibit very competitive properties while still being recyclable.[3−5] TPEs are widely used in various sectors of modern production as adhesives, automotive components, coatings, fibers, electronics, etc.[6,7] Almost all TPEs contain two or more distinct polymeric phases, encompassing incompatible soft [glass transition temperature (T_g) < RT] and hard [T_g or melting temperature (T_m) > RT] phases that form nanodomains with controlled sizes and geometries.[8−10] Hard polymer domains function as thermally stable anchors. The other phase is composed of soft amorphous segments, which contribute to the rubbery properties. From this segregated state, a homogeneous material can be reformed provided that the polymer is heated above its characteristic order−disorder transition temperature (T_{ODT}). The synthesis of these elastomers, either by chain-growth or by step-growth polymerization, results in a wide spectrum of materials. They usually consist of copolymers with various macromolecular structures, e.g., random,[11] graft,[12] star,[13] and ABA (hard−soft−hard) triblock copolymers.[14] Varying the ratio of hard and soft segments allows the design of materials with tailor-made properties.

Styrenic block copolymers (SBCs) are a well-known family of TPEs that are industrially available under the Kraton trademark.[15] SBCs are synthesized via sequential anionic copolymerization of styrene and dienes and have found interest in applications owing to their unique properties and low cost. However, they suffer from several drawbacks, such as sensitivity to UV and oxidation due to the presence of unsaturations in the rubbery phase.[4] In addition, this class of TPEs has a limited service temperature range due to the relatively low T_g of the styrenic phase (≈100 °C). Some efforts have been undertaken to increase the upper service temperature of SBCs by introducing adamantyl[16−18] or 1,1-diphenylethylene[19,20] groups, which changes the polymerization conditions and can have a significant influence on the

Received: May 31, 2024
Revised: September 13, 2024
Accepted: September 23, 2024
Published: October 2, 2024

https://doi.org/10.1021/acs.macromol.4c01233
Macromolecules 2024, 57, 9565−9575

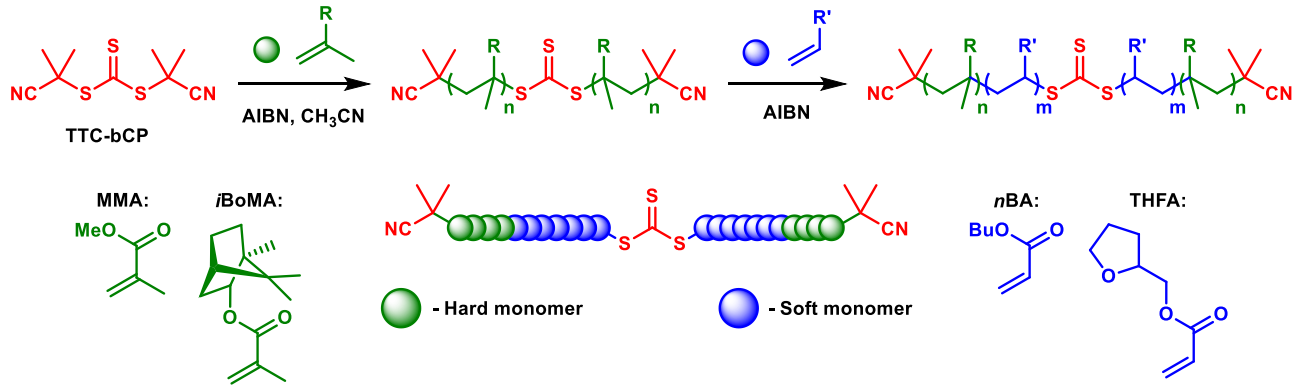

Figure 1. General scheme describing the synthesis of ABA triblock copolymers using the **TTC-bCP** RAFT agent.

Table 1. Experimental Conditions and Results of TTC-bCP-Mediated RAFT Polymerization of Methacrylates[a]

entry	[M]/[CTA]/[I]	monomers	time, h	conversion, %[b]	$M_{n(theor)}$ kg mol^{-1}[c]	$M_{n(SEC)}$, kg mol^{-1}[d]	$Đ$ (M_w/M_n)[d]
1[f]	330/1/0.3	MMA	1.5	8.5	3.0	4.5	1.26
2	330/1/0.3	MMA	4.5	23.7	8.0	8.6	1.24
3	330/1/0.3	MMA	8	40.7	13.5	13.3	1.21
4	330/1/0.3	MMA	18	72.4	23.8	23.2	1.15
5	330/1/0.3	MMA	25	94.3	31.0	29.8	1.12
6	330/1/0.3	MMA	40	99.9	32.8	31.2	1.12
7	450/1/0.3	MMA	28	92.6	42.3	39.0	1.10
8	1100/1/0.3	MMA	70	99.0	112	112	1.11
9	330/1/0.3	*i*BoMA	2	11.5	8.3	18.7	1.25
10	330/1/0.3	*i*BoMA	5	41.9	29.7	40.1	1.19
11	330/1/0.3	*i*BoMA	9	66.6	47.0	59.8	1.29
12	330/1/0.3	*i*BoMA	24	97.7	68.8	75.9	1.24
13[e]	330/1/0.3	*i*BoMA	17	46.2	33.7	45.5	1.28
14	(125/125)/1/0.3	MMA/*i*BoMA	2	13.8	6.0	11.1	1.32
15	(125/125)/1/0.3	MMA/*i*BoMA	5	37.5	15.8	21.3	1.12
16	(125/125)/1/0.3	MMA/*i*BoMA	8	56.9	23.9	29.4	1.12
17	(125/125)/1/0.3	MMA/*i*BoMA	15	72.2	30.3	34.2	1.13
18	(125/125)/1/0.3	MMA/*i*BoMA	22.5	97.6	40.8	47.8	1.09
19	(46/138)/1/0.3	MMA/*i*BoMA	28	100	44.6	41.7	1.13

[a]Reaction conditions: CTA = **TTC-bCP**, I = AIBN, temperature = 60 °C, monomer concentration = 70 wt % (in MeCN for MMA, and in PhMe for MMA/*i*BoMA and *i*BoMA). [b]Determined by ^{1}H NMR. [c]Determined by the following equation: $M_{n(theor)} = [m_{(mon.)} \times conv._{(mon.)} \times M_{(RAFT\ agent)}/m_{(RAFT\ agent)}] + M_{(RAFT\ agent)}$. [d]Determined by SEC-RI-MALS in THF. [e]Polymerization performed in a Schlenk flask on the 1.5 g scale for the synthesis of the triblock copolymer. [f]Data of entry 1−6 taken from ref 33.

interaction parameter, χ, with respect to polydienes. In this regard, poly(meth)acrylate-based TPEs have the potential to replace traditional SBCs for some applications, where optical properties and durability are important as well as the need to increase the upper service temperature without impairing the elastomeric properties. High T_g materials can be more easily obtained by statistical copolymerization of common methyl methacrylate (MMA) monomer ($T_{g(PMMA)} \approx 100$ °C)[21] with commercially available methacrylates of higher T_g such as isobornyl methacrylate (*i*BoMA, $T_{g(PiBoMA)} \approx 190-200$ °C).[22] Regarding the soft block, poly(*n*-butyl acrylate) (P*n*BA, $T_{g(PnBA)} \approx -54$ °C)[23] is widely used in the context of all-(meth)acrylic TPEs.[24]

These materials were recently developed on the industrial scale by Kuraray using living anionic polymerization (LAP).[25] There were several reports for the synthesis of such TPEs by reversible-deactivation radical polymerization (RDRP) methods, such as nitroxide-mediated polymerization by Arkema,[26] atom transfer radical polymerization,[27] and reversible addition−fragmentation chain transfer (RAFT)[28,29] polymerization. However, RDRP methods were unable to compete with the LAP process, which showed superior control over the macromolecular architecture and resulted in polymers with lower dispersities.[27,28]

Until recently, all the RAFT approaches considered to produce (meth)acrylic hard−soft−hard ABA triblocks suffered from strong limitations due to the low reactivity of available symmetrical RAFT agents toward methacrylates. Indeed, trithiocarbonates (TTCs) with tertiary leaving groups such as carboxy or ester functions resulted in relatively ill-defined triblock copolymers with dispersity $Đ > 1.5$.[29−32] Recently, our group filled this gap by synthesizing a new symmetrical TTC (**TTC-bCP**) comprising 2-cyanopropan-2-yl groups known to provide an optimal fragmentation rate for methacrylate monomers.[33] For the first time, a low dispersity ($Đ < 1.1$) PMMA-*b*-P*n*BA-*b*-PMMA triblock copolymer, with a relatively high number-average molar mass (M_n) value was synthesized by a convergent RAFT process in two steps. The copolymer exhibited a dispersity comparable to those of its counterparts derived from LAP.

In this work, the **TTC-bCP** RAFT agent was used to synthesize all-(meth)acrylic triblock copolymers (Figure 1)

https://doi.org/10.1021/acs.macromol.4c01233
Macromolecules 2024, 57, 9565−9575

with tunable hard and soft phases with enhanced service temperature and biobased content. To do so, *i*BoMA was used either as a single hard monomer or as comonomer with MMA for the polymerization of the hard block. In addition, the biobased tetrahydrofurfuryl acrylate (THFA) was evaluated as a soft monomer. Narrowly dispersed methacrylate-acrylate-methacrylate triblock copolymers of controlled high molar masses were synthesized and resulted in materials with modulated T_g values and stable thermoplastic elastomeric (TPE) properties over an extended range of temperature inherent to the formation of segregated microdomains.

EXPERIMENTAL SECTION

Materials. Methyl methacrylate (MMA, Aldrich, 99%), *n*-butyl acrylate (*n*BA, Aldrich, 99%), and *i*BoMA (Aldrich, technical grade) were purified by passing through a basic alumina column. Tetrahydrofurfuryl acrylate (THFA, Aldrich, 99%) was purified by vacuum distillation. 2,2′-Azobis(2-methylpropionitrile) (AIBN, Aldrich, 99%) was purified by recrystallization in methanol. 2,2′-Azobis(4-methoxy-2,4-dimethylvaleronitrile) (V-70, 95%), tetrahydrofuran (THF, Aldrich, HPLC grade), toluene (PhMe, Aldrich, 99%), acetonitrile (MeCN, Fisher, HPLC grade), acetone (Me_2CO, Aldrich, HPLC grade), petroleum ether (Aldrich, ACS reagent), methanol (MeOH, Aldrich, HPLC grade), 2-aminopropane (*i*Pr-NH_2, Aldrich, Aldrich, 99%), and 1,3,5-trioxane (Triox, Aldrich, 99%) were used as received.

Characterization. *Nuclear Magnetic Resonance.* ^{1}H and ^{13}C nuclear magnetic resonance (NMR) spectra were recorded on a Bruker AV 300 MHz spectrometer. Deuterated chloroform was used as a solvent and reference in all samples ($CDCl_3$, δ = 7.26 ppm). Chemical shifts are given in parts per million (ppm).

Size Exclusion Chromatography. Number-(M_n) and weight-average (M_w) molar masses and corresponding dispersities ($Đ$) were determined by size-exclusion chromatography (SEC) on a system composed of a Waters 515 HPLC pump, an Agilent 1260 autosampler, a Varian ProStar 500 column valve module, a set of three Waters columns (Styragel Guard Column, 20 μm, 4.6 mm × 30 mm, Styragel HR3, 5 μm, 7.8 mm × 300 mm and Styragel HR4E, 5 μm, 7.8 mm × 300 mm), a Varian ProStar 325 UV−vis detector set at 290 nm, Wyatt Optilab rEX differential refractive index detector, and a Wyatt MiniDawn TREOS multiangle light scattering detector. Tetrahydrofuran (THF) was used as eluent for all samples at a flow rate of 1.0 mL/min (35 °C). Samples were diluted to a concentration of about 5 mg/mL and filtered through 0.45 μm Nylon syringe filters before injection. The column system was calibrated with PMMA standards (ranging from 0.96 to 265.3 kg mol^{-1}) for the determination of the average molar masses of one single low molar mass PMMA sample (Table 1, entry 1). For all of the other polymers, average molar masses were determined using RI-MALS detection. The following refractive index increment (d*n*/d*c*) values were used: $(dn/dc)_{PMMA}$ = 0.085,[34] $(dn/dc)_{PnBA}$ = 0.067,[35] $(dn/dc)_{PiBoMA}$ = 0.108,[36] and $(dn/dc)_{PTHFA}$ = 0.085.[37] Average molar masses were determined using Astra software.

Differential Scanning Calorimetry. The glass transition temperature (T_g) of the polymers was measured by differential scanning calorimetry (DSC) using Mettler Toledo STARe DSC in a nitrogen atmosphere using aluminum crucibles of 40 μL at heating rates of 10 °C/min. Samples in 5−10 mg portions were used for all analyses. All T_g values were obtained from the second or third ramps to remove the thermal history of the samples.

Thermogravimetric Analysis. TGA analyses were conducted on a TGA/DSC 3+ Mettler instrument with a temperature ramp of 10 °C/min under N_2 (50 mL/min).

Dynamical Mechanical Analysis. Isochronal temperature ramp tests were performed on an Anton Paar MCR 302. The experiments were performed in parallel plate geometry using 8 mm sample disks. A frequency of 1 rad s^{-1}, and a strain of 1% were used to record the evolution of the dynamic moduli as a function of the temperature with a heating rate of 2.5 °C/min.

Small Angle X-ray Scattering. Small angle X-ray scattering (SAXS) experiments were performed after thermal annealing under vacuum at 180 °C for 8 h. SAXS data were acquired in transmission mode on a high-resolution X-ray spectrometer Xeuss 2.0 (Xenocs) operating with a radiation wavelength of λ = 1.54 Å at 25°C and 150 °C. The resulting 2D images were found to be isotropic, and the data were azimuthally averaged to yield curves of the scattering intensity, $I(q)$, as a function of the scattering vector, q. The beam center position and the angular range were calibrated using silver behenate as the standard.

Synthesis. *RAFT Agent Synthesis (**TTC-bCP**).* Bis(2-methylpropanenitrile)-trithiocarbonate (**TTC-bCP**) was prepared following an adaptation of our previously published procedure.[33] A solution of 2-mercapto-2-methylpropanenitrile (200 mg, 1.98 mmol) in 5 mL of dry MeCN was purged with argon and added slowly (dropwise) during 2 h to a solution of 1,1′-thiocarbonyldiimidazole (171 mg, 0.96 mmol) in 5 mL of dry MeCN purged with argon. The reaction mixture was allowed to stir for an additional hour. A change in color of the reaction solution was observed from yellow to bright orange. Upon completion, the reaction mixture was transferred on the silica column under argon. **TTC-bCP** was recovered from column chromatography under an argon atmosphere (50% ethyl acetate/50% cyclohexane R_f = 0.9). After column purification, the purity was about 90% (10% of disulfide impurity), and the yield was 68%. To obtain a 99.9% pure compound, a recrystallization from $CHCl_3$/*n*-pentane was necessary.

^{1}H NMR (300 MHz, $CDCl_3$, δ): (ppm): 1.91 (s, 6H, S−C$(CH_3)_2$−CN). ^{13}C NMR (75 MHz, $CDCl_3$): δ (ppm): 211.01 (S−(C═S)−S); 119.70 (CN); 42.93 (S−C$(CH_3)_2$−CN); 26.95 (S−C$(CH_3)_2$−CN).

Polymerization Procedure. The initiator, RAFT (or polymethacrylate macro-RAFT) agent, solvent (if needed), and monomer were mixed, and the obtained solution was divided in ampules (or Schlenk flasks), which were sealed after degassing by three freeze−pump−thaw cycles and immersed in an oil bath at different temperatures for the desired time. The polymerization was stopped by rapid cooling, and the solution was immediately transferred to NMR tubes for conversion analysis. The remaining solution was dried under a vacuum and used as such for the preparation of SEC samples. Monomer conversions were calculated by the integrations of vinyl protons compared either to polymer or to the 1,3,5-trioxane standard (≈5.2 ppm). The polymers were purified by precipitation. The crude polymer was dissolved in the minimum amount of good solvent (Me_2CO for PMMA, MePh for others), and the resulting viscous oil was slowly added dropwise into a nonsolvent in excess (petroleum ether for PMMA, MeOH for others). The obtained solid polymer was then filtered, washed, and dried under vacuum. For some samples, the procedure was repeated several times to remove traces of the residual monomer.

Using the procedure described above, a typical polymerization was conducted as follows (Table 3, entry 1). AIBN (0.001 mmol, 0.17 mg), PMMA macro-RAFT agent (Table 1, entry 7) (0.01 mmol, 0.4 g), and *n*BA (8.64 mmol, 1.1 g) were mixed. The solution was transferred to a glass ampule, which was flame-sealed after degassing by three freeze−pump−thaw cycles and immersed in an oil bath at 60 °C for 20 h. The polymerization was stopped by rapid cooling. After opening, the solution was immediately transferred to an NMR tube for conversion analysis (86.6%). The volatiles were removed by evaporation. The crude product was dissolved in PhMe and precipitated in MeOH.

^{1}H NMR (300 MHz, $CDCl_3$, δ): (ppm): 1. PMMA part: 3.60 (s, 3H, O−CH_3), 1.82−2.02 (m, 2H, CH_2), 0.85−1.25 (s, 3H, CH_3); 2. P*n*BA part: 4.03 (s, 2H, O−CH_2), 1.90−2.28 (s, H, CH_2−CH−$COOCH_2$−), 1.55−1.62 (m, 2H, O−CH_2−CH_2−CH_2−CH_3), 1.49 (m, 2H, CH_2−CH−$COOCH_2$−), 1.31−1.43 (m, 2H, O−CH_2−CH_2−CH_2−CH_3), 0.91−0.96 (m, 3H, O−CH_2−CH_2−CH_2−CH_3). M_n = 174 kg mol^{-1}, and $Đ$= 1.05.

https://doi.org/10.1021/acs.macromol.4c01233
Macromolecules 2024, 57, 9565−9575

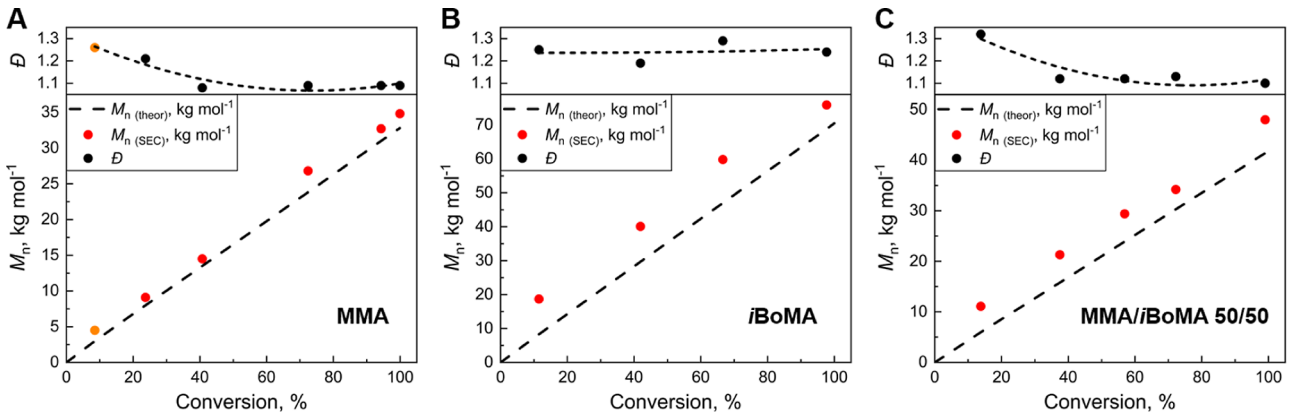

Figure 2. M_n and $Đ$ vs conversion during methacrylate RAFT polymerization with **TTC-bBP** at 60 °C. Values were determined by SEC-MALS in THF (except for the lowest conversion data (orange symbols) where PMMA calibration has been used). MMA (A), *i*BoMA (B), and MMA/*i*BoMA (50/50 mol.%) (C). Polymerization conditions are reported in Table 1. Data for A taken from ref 33.

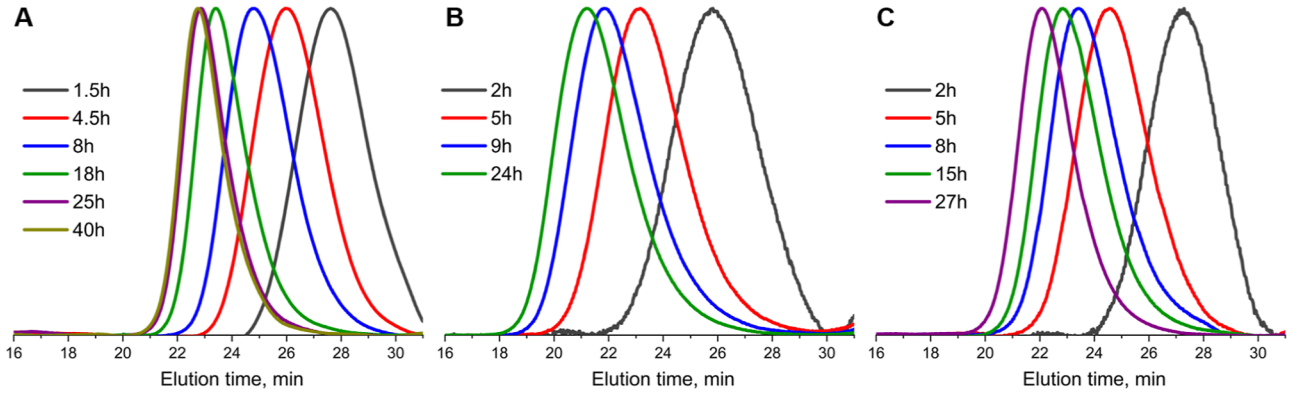

Figure 3. SEC-RI chromatograms of MMA (A), *i*BoMA (B), and *i*BoMA/MMA (50/50) (C) polymerization in the presence of **TTC-bCP** as the RAFT agent. Polymerization conditions of Table 1. Data for A taken from ref 33.

NMR of polymers is presented in the Supporting Information (Figures S3–S7).

RESULTS AND DISCUSSION

Hard Block Synthesis. In a first communication,[33] the newly proposed symmetrical RAFT agent **TTC-bCP** (Figure 1) showed excellent efficiency for the preparation of one single PMMA-*b*-P*n*BA-*b*-PMMA triblock copolymer with very good control over molar masses and remarkably low dispersities ($Đ$= 1.04). The control and polymer definition offered by this RAFT agent was unprecedented compared to classically used symmetrical RAFT agents such as *S*,*S*′-bis(*α*,*α*′-dimethylacetic acid)trithiocarbonate.[31] To better evaluate the potential of this RAFT agent for the design of TPE materials of higher and tunable service temperature, *i*BoMA was considered as high T_g monomer ($T_{g(iBoMA)}$ = 190–200 °C), either alone or as a MMA/*i*BoMA 50/50 (mol %) feed composition for a targeted M_n of 30 kg mol^{-1}. Results were compared to PMMA synthesis taken as a reference. Polymerizations were followed by ^{1}H NMR to determine methacrylate conversion and SEC to follow the evolution of average molar masses (Table 1).

MMA polymerization was well-controlled with a linear evolution of M_n with conversion and a gradual decrease of dispersity values down to 1.10 during polymerization (Table 1, entry 1–7, Figure 2A).[33] M_n values determined by SEC-RI-MALS analysis were in excellent agreement with those expected for a controlled process, suggesting negligible irreversible termination or transfer reactions. This observation was confirmed by monomodal chromatograms obtained by SEC over the whole range of conversions (Figure 3A). To evaluate the possibility of controlling RAFT polymerization of MMA for much higher M_n, a PMMA of 110 kg mol^{-1} was targeted (Table 1, entry 8). Satisfactorily, a comparable level of control was obtained with a M_n of 112 kg mol^{-1} ($M_{n(theor)}$ = 112 kg mol^{-1}) and a dispersity of 1.11.

P*i*BoMA possesses interesting characteristics such as a much higher T_g than PMMA (190–200 °C vs 100 °C) and is partially biosourced as isoborneol is a terpene derivative. Surprisingly, studies reporting the RAFT homopolymerization of *i*BoMA are rare and showed only moderate control over polymerization.[38] Therefore, RAFT polymerization of *i*BoMA was conducted with RAFT agent **TTC-bCP** (Table 1, entry 9–13). Using our conditions with 70 wt.% monomer in PhMe at 60 °C with AIBN initiation, dispersities obtained for P*i*BoMA ($Đ$= 1.19–1.29) are among the lowest reported for this monomer by RDRP[39] (Figure 2B). However, dispersities are higher than for PMMA (1.24 versus 1.10 at a conversion >97%). This increase in dispersity could be related to the relatively high steric hindrance of the isobornyl group compared to methyl in MMA, which could decrease the transfer constant of P*i*BoMA propagating radicals to **TTC-bCP**. Nonetheless, monomodal chromatograms were obtained. A linear increase in M_n with conversion was observed, while M_n values were slightly greater than theoretical ones (Figure 3B). The overall higher reactivity of *i*BoMA compared to MMA can be mostly explained by the greater polymerizability of *i*BoMA.

https://doi.org/10.1021/acs.macromol.4c01233
Macromolecules 2024, 57, 9565–9575

Table 2. Experimental Conditions and Results of TTC-bCP-Mediated RAFT Polymerizations of Acrylates[a]

entry	[M]/[CTA]/[I]	monomers	time, h	conversion, %[b]	$M_{n(theor)}$, kg mol^{-1}[c]	$M_{n(SEC)}$, kg mol^{-1}[d]	$Đ$ (M_w/M_n)[d]
1[e]	330/1/0.3	*n*BA	1	2.0	1.1	2.3	1.37
2	330/1/0.3	*n*BA	1.5	18.0	7.9	10.1	1.08
3	330/1/0.3	*n*BA	2	42.3	18.3	17.4	1.06
4	330/1/0.3	*n*BA	3	68.2	29.3	28.1	1.05
5	330/1/0.3	*n*BA	6	88.2	37.8	35.7	1.06
6	330/1/0.3	*n*BA	9	94.3	40.4	34.3	1.10
7	1500/1/0.1	*n*BA	1	1.0	2.1	4.7	1.40
8	1500/1/0.1	*n*BA	1.5	6.1	11.6	10.7	1.21
9	1500/1/0.1	*n*BA	8	55.7	104	95.7	1.03
10	1500/1/0.1	*n*BA	13	67.5	125	120	1.03
11	1500/1/0.1	*n*BA	24	83.5	155	141	1.02
12	1500/1/0.1	THFA	1	22	50.3	62.8	1.29
13	1500/1/0.1	THFA	1.5	40	91.2	97.0	1.40
14	1500/1/0.1	THFA	2	58	132	184	2.13
15	1500/1/0.1	THFA	4	90	205	247	26.34

[a]Reaction conditions: CTA = **TTC-bCP**, I = AIBN (entry 1−11) or V-70 (entry 12−15), temperature = 60 °C (entry 1−11), 30 °C (entry 12−15), monomer concentration = 70 wt % in PhMe for entry 1−6 and bulk for entry 7−15. [b]Determined by ^{1}H NMR. [c]Determined by the following equation: $M_{n(theor)}=(m_{(mon.)} \times conv._{(mon.)} \times M_{(RAFT\ agent)}/m_{(RAFT\ agent)}) + M_{(RAFT\ agent)}$. [d]Determined by SEC-RI-MALS in THF. [e]Entry 1−6 taken from ref 33.

Indeed, it was reported that the propagation rate constant k_p of MMA in bulk at 60 °C equals 830 L mol^{-1} s^{-1},[40] while k_p = 1436 L mol^{-1} s^{-1} for *i*BoMA.[41] In addition, it can be assumed that the termination rate constant k_t of *i*BoMA is lower than that of MMA due to steric considerations. Finally, the fact that the nature of the polymerization solvent (MeCN for MMA and PhMe for *i*BoMA) may have an effect on the rate of polymerization cannot be ruled out.

Controlling the T_g of the hard block is an important objective since a too high T_g such as the one of P*i*BoMA might be irrelevant for all-(meth)acrylic TPE materials as it would impose even higher processing temperatures, which may be too close to the degradation temperature of polymethacrylates. Therefore, an improperly adjusted T_g of the outer hard blocks could potentially restrain the use of common processing techniques usually found in thermoplastics, such as extrusion or injection molding. As a consequence, the RAFT polymerization of the MMA/*i*BoMA mixtures was also evaluated. According to the Kwei equation,[42] a T_g value in the range of 100−200 °C is expected for an *i*BoMA content between 0% and 100% of *i*BoMA.[43] A feed ratio of 50/50 (mol %) MMA/*i*BoMA was first selected as it provides intermediate T_g. By following monomer consumptions by ^{1}H NMR, it was found a MMA and *i*BoMA are isoreactive throughout the reaction (Figures S8 and S9), thus forming a copolymer with statistical composition. Control of M_n and $Đ$ values was in the same order that MMA polymerization, showing a strong beneficial effect of the MMA comonomer in *i*BoMA polymerization (Figures 2C and 3C, and Table 1, entry 14−18). This implies that the propagating radicals preferably transfer to **TTC-bCP** through MMA[44] radicals, resulting in an overall greater apparent transfer constant, resulting in a better polymerization control. The linear increase of M_n with conversion was observed, while M_n values were slightly greater than theoretical ones but were intermediate between those obtained for pure PMMA and P*i*BoMA. Nonetheless, a T_g of 131 °C was obtained for 50/50 MMA/*i*BoMA polymerization, close to the T_g of pure PMMA. Thus, a polymerization of 25/75 MMA/*i*BoMA was also conducted (Table 1, entry 19) and resulted in a T_g of 155 °C (see the Thermal Properties section for detailed discussion). Thus, MMA/*i*BoMA comonomer mixtures were also selected for the preparation of ABA triblock copolymers with various T_g values of the hard phase.

Soft Block (Homopolymer) Synthesis. RAFT homopolymerizations of *n*BA and THFA monomers were first studied with **TTC-bCP** in toluene to optimize the polymerization conditions for the synthesis of the soft midblock. As we previously discussed,[33] polymerization of *n*BA was much faster than that of MMA under similar conditions (Table 2, entry 1−6), owing to the greater intrinsic reactivity of *n*BA, although an induction time of about 1 h is noteworthy (Table 2, entry 1−6). A linear evolution of M_n with conversion and excellent match of values with those estimated for a controlled RAFT process was observed. Dispersities are low, with values down to 1.06 after 88% conversion, and with a slight increase to 1.10 after 94% conversion, suggesting a minor contribution of chain transfer to solvent as evidenced by the appearance of a shoulder in the lower molar mass area of the corresponding chromatograms (Figure S10, 9 h).

To evaluate the influence of solvent regarding the occurrence of side reactions, polymerization of *n*BA was carried out in toluene at different dilutions. We applied relative *n*BA/**TTC-bCP**/AIBN concentration conditions of 800/1/0.1 as it is typical for the targeted length of the soft block during chain extension from polymethacrylate-**TTC-bCP** (see Triblock Copolymer Synthesis section). *n*BA conversion after 7 h of reaction at 60 °C reaches 85.9, 72.2, and 67.1% for 77 wt % of *n*BA in toluene, 50 wt %, and bulk conditions, respectively (Table S1, entry 1−3). The use of a limited amount of solvent decreases the viscosity of the reaction medium and improves the reactant diffusion, allowing access to higher conversion in comparison to bulk, but an increase in dilution slows down the polymerization kinetics as expected. Noteworthy, a marked bimodal molar mass distribution is obtained in solution polymerization in contrast to bulk polymerization (Figure S11). The peak mass M_p of the population of lower mass is roughly half of that of the main population. These observations are characteristic of chain transfer to solvent occurring in a RAFT process using a symmetrical RAFT agent with a Z-group approach, for which deactivated polymer chains have roughly

https://doi.org/10.1021/acs.macromol.4c01233
Macromolecules 2024, 57, 9565−9575

half the length of the main RAFT population. For this reason, the syntheses of triblock copolymers were all conducted in bulk.

On the basis of literature, a hard/soft molar ratio of 2:5 (1 hard-5 soft-1 hard)[45] with M_n of PMMA segments higher than 10 kg mol^{-1} is suited to give materials with good TPE properties. Due to the incomplete polymerization of *n*BA in bulk as a result of the high viscosity of the medium, the reaction was conducted with a *n*BA to RAFT agent ratio of 1500 (Table 2, entry 7−11) for the later targeted PMMA$_{20K}$-P*n*BA$_{100K}$-PMMA$_{20K}$ structure. Relatively high molar masses were targeted in order to induce enough chain entanglement and therefore good mechanical properties.[46] An excellent control of the polymerization was obtained with the control of M_n with a well-defined molar mass distributions and dispersities as low as 1.02 (Figure 4). The desired molar mass of about 125 kg mol^{-1} was obtained after polymerization for 13 h of polymerization.

In addition to *n*BA, THFA, a biobased monomer, was also evaluated as constituting soft block (T_g = −11 °C).[37] Standard conditions of 60 °C with AIBN provided poor RAFT control, probably due to the presence of many acidic protons, which are prone to transfer reactions inducing branching and eventually cross-linking reactions (Table S1, entry 4−8). Reasonably good M_n control with low dispersities ($Đ$ = 1.25) was solely obtained at conversions up to 30%, making this monomer unlikely suitable for the preparation of TPE materials. V-70 initiation at 30 °C was considered with the idea of reducing the contribution of side reactions (Table 2, entry 12−15). Under these initiation conditions in bulk and for THFA conversions not greater than 40%, the best control ever reported for this monomer using a RDRP approach was achieved. Indeed, monomodal SEC chromatograms were obtained (Figure S12, 1.5 h) with M_n of 97 kg mol^{-1} and $Đ$ = 1.40 at 40% conversion. THFA has already been used to create poly(1-adamantyl acrylate)-*b*-poly(tetrahydrofurfuryl acrylate)-*b*-poly(1-adamantyl acrylate) triblock copolymer with TPE properties by RAFT polymerization.[28] However, the best dispersity achieved was 1.66 with a relatively short soft block of 23 kg mol^{-1} and a bimodal peak observed in SEC. Another possibility to reduce dispersity may have been to copolymerize THFA statistically with *n*BA (Table S1, entries 9−13), but no significant improvement was noticed.

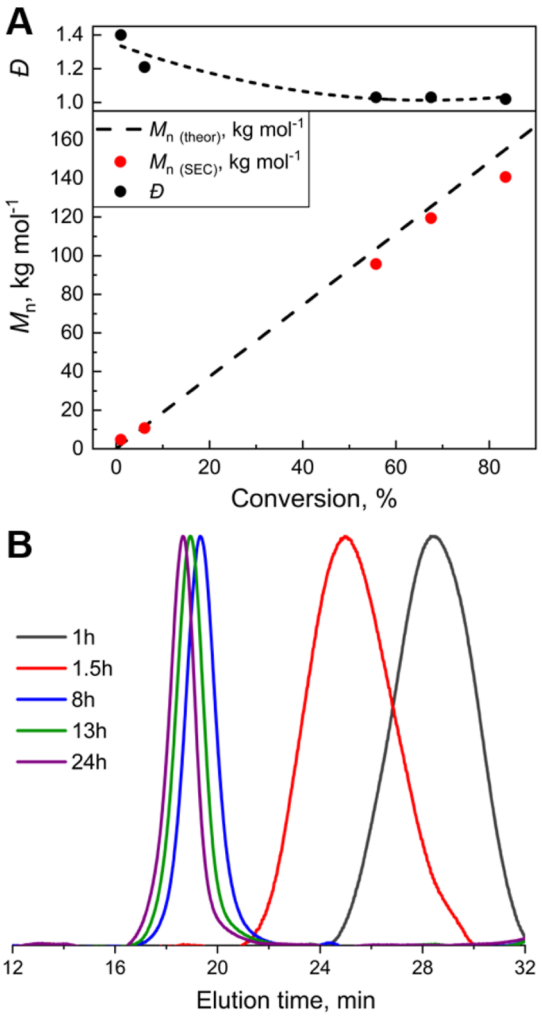

Figure 4. M_n and $Đ$ vs conversion (A) and corresponding SEC-RI chromatograms (B) of *n*BA polymerization with **TTC-bCP** as the RAFT agent at 60 °C in bulk.

Triblock Copolymer Synthesis. PMMA-*b*-P*n*BA-*b*-PMMA triblock copolymers were synthesized according to the optimized conditions reported above for both monomers. Chain extension from a PMMA macro-CTA (Figure 5A) with M_n of 39 kg mol^{-1} showed a clear shift of the chromatogram toward a higher molar mass of 174 kg mol^{-1}, proving the successful chain extension. Dispersity values decreased to 1.05 over time, reflecting the excellent control of the polymerization (Table 3, entry 1). In order to confirm the formation of a symmetrical triblock structure, the copolymer was reacted with isopropylamine. This reaction induces the cleavage of C−S bonds, resulting in the formation of the corresponding PMMA-*b*-P*n*BA diblock copolymer. This is clearly seen by SEC analysis, where the molar mass of the triblock copolymer is divided by two after aminolysis (see chromatograms and conditions in Figure S13).

The efficiency of chain extension was also verified for higher molar masses. To do so, a reaction with [*n*BA]/[PMMA-**TTC-bCP**] = 15 000 was carried out, which corresponds to a targeted M_n of about 2000 kg mol^{-1} for the triblock copolymer, starting from a PMMA macro-CTA of 112 kg mol^{-1} (Table 3, entry 2). The chain extension was successful, leaving no residual PMMA precursor. The shape of the peak remained monomodal but slightly broadened as a result of a long polymerization time (30 h) and possible side reactions after 63.9% conversion (Figure S14). Nevertheless, a PMMA-*b*-P*n*BA-*n*-PMMA triblock copolymer with an ultrahigh molar mass of about 2000 kg mol^{-1} and relatively low dispersity ($Đ$ = 1.43) was prepared. Overall, access to very high controlled M_n and still relatively low dispersity is afforded owing to both extremely good control of the polymerization offered by **TTC-bCP** and optimized polymerization conditions responsible for minimized side reactions. Such a level of high molar mass control was only reported in the case of photomediated RAFT polymerization,[47] emulsion[48,49] or gel polymerization,[50] or by RAFT polymerization at very high pressures.[51]

Higher T_g P*i*BoMA-*b*-P*n*BA-*b*-P*i*BoMA triblock copolymers were also prepared (Table 3, entry 3−4). Starting from a P*i*BoMA-**TTC-bCP** macro-CTAs, shifts in chromatograms are clearly visible for two different molar masses of the soft midblock, with M_n in agreement with expected values and a significant decrease in dispersity down to 1.02 (Figure 5B). In the same way, a well-defined P(*i*BoMA-*co*-MMA)-*b*-P*n*BA-*b*-

https://doi.org/10.1021/acs.macromol.4c01233
Macromolecules 2024, 57, 9565−9575

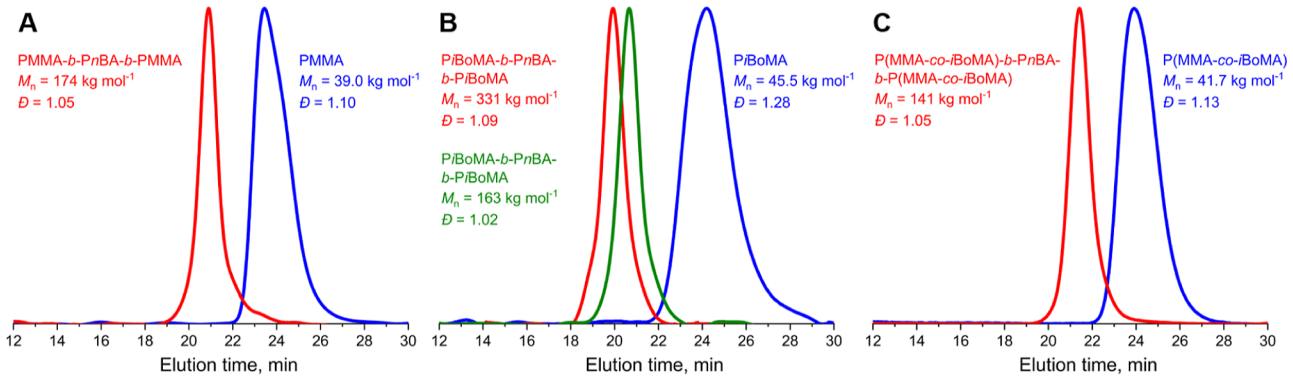

Figure 5. SEC-RI chromatograms of triblock copolymers and corresponding methacrylate macro-CTAs. (A) PMMA-*b*-P*n*BA-*b*-PMMA (Table 3, entry 1), (B) P*i*BoMA-*b*-P*n*BA-*b*-P*i*BoMA (Table 3, entry 3 and 4), and (C) P(MMA-*co*-*i*BoMA)-*b*-P*n*BA-*b*-P(MMA-*co*-*i*BoMA) (Table 3, entry 5).

P(*i*BoMA-*co*-MMA) with a controlled M_n of about 140 kg mol^{-1} and a low $Đ$ of 1.05 was synthesized (Table 3, entry 5, and Figure 5C).

We evaluated the possibility to synthesize a fully biobased P*i*BoMA-*b*-PTHFA-*b*-P*i*BoMA copolymer. The synthesis of triblock copolymers from P*i*BoMA-**TTC-bCP** with THFA was difficult since it was necessary to stop the reaction before the generation of polymer branching. Still, monomodal peaks were observed only at around 15% conversion for the synthesis of P*i*BoMA$_{23k}$-*b*-PTHFA$_{34k}$-*b*-P*i*BoMA$_{23k}$ (Table 3, entry 6) with a monomodal SEC chromatogram (Figure S15) and an acceptable $Đ$ of 1.31. However, it was decided not to study the TPE properties of this class of copolymer due to the insufficient length of the PTHFA soft block.

Thermal Properties. The T_g values were measured by DSC (Table 4 and Figure S17A). In our previous study,[33] starting from polymethacrylates-**TTC-bCP**, a T_g of 121 °C (instead of the expected 100 °C) was observed for PMMA. A similar value has already been reported for some PMMA-based acrylic block copolymers.[52] On the contrary, for P*i*BoMA, the T_g value of 181 °C was lower than anticipated (190−200 °C according to literature).[22] For P(*i*BoMA-*co*-MMA), the dependence of T_g values on the copolymer composition is known to be not linear.[43] That is why for a *i*BoMA/MMA composition of 50/50 mol %, a T_g value of 131 °C was obtained, while for *i*BoMA/MMA = 75/25, a higher T_g of 155 °C was achieved, which is in close agreement with literature.[43]

Due to the relatively low weight fraction of the hard block, the observation of the T_g of the hard block in triblock copolymers was not always possible (Figure S17B). This is especially true for P*i*BoMA, which contains much less monomer units in comparison to a PMMA of similar molar mass due to the molecular weight of the *i*BoMA monomer being more than twice as high as that of MMA. The fact that T_g values of the hard block of PMMA-*b*-P*n*BA-*b*-PMMA and P(MMA-*co*-*i*BoMA)-*b*-P*n*BA-*b*-P(MMA-*co*-*i*BoMA) hardly differed from those of polymethacrylate-**TTC-bCP** precursors, with T_g of the soft block being very close to that of *n*BA homopolymer, hinted a proper microphase separation between the blocks (Table 4, entry 5−9).

The thermal stability of the polymers was tested using TGA under air and an inert atmosphere (Figure S16). PMMA-**TTC-bCP** showed the lowest stability with a 5% weight loss at 175 °C. Similar results were previously obtained for PMMA with TTC end groups.[53] In contrast, P*n*BA-**TTC-bCP** was much more thermally stable, with a 5% weight loss at 305 °C. The PMMA-*b*-P*n*BA-*b*-PMMA triblock copolymer, with midchain TTC groups surrounded by a P*n*BA environment, exhibits stability similar to P*n*BA, with a 5% weight loss reached at 257 and 295 °C in air and in an inert atmosphere, respectively, which shows good potential for applications as TPE materials. The TGA data obtained are in good agreement with the results of a similar triblock copolymer synthesized by LAP by Kuraray[54] (5% loss at 276 and 316 °C in air and in an inert atmosphere, respectively), which shows the competitiveness of the RAFT process in relation to more stringent anionic polymerization. It is important to note that quantitative assessment of TTC stability in such triblock copolymers is not possible by TGA due to its low weight fraction (<0.1%).

RAFT thiocarbonylthio groups are known to exhibit limited thermal stability at high temperatures. This stability is strongly dependent on the chemical nature of the Z-stabilizing group and the neighboring groups. It was reported that TTC elimination can be achieved at temperatures above 200 °C for P*n*BA-TTC.[55] To evaluate the possible negative impact of the TTC group on TPE properties, the PMMA$_{20k}$-*b*-P*n*BA$_{135k}$-*b*-PMMA$_{20k}$ triblock copolymer was heated five times at 180 °C for 30 min in an air atmosphere. The 180 °C value was selected arbitrarily because TTC degradation is likely to be triggered around this temperature for polyacrylates.[55] A slight broadening of the molar mass distribution (from $Đ$ = 1.05 to 1.07) without a significant change of M_n of the heat-treated sample was observed (Figure 6), attesting the good stability of the TTC link under these conditions.

The thermal stability of PMMA$_{20k}$-*b*-P*n*BA$_{135k}$-*b*-PMMA$_{20k}$ was also investigated through an isothermal treatment at 180 °C for 30 min, followed by measurements of the storage modulus between 20 and 100 °C. This cycle was repeated five times. Indeed, the cleavage of the midchain TTC group would generate a fraction of a diblock copolymer with dangling P*n*BA blocks in the triblock copolymer, strongly deterring the envisioned TPE properties. Figure S18 shows that such thermal treatment has no influence on the viscoelastic properties of PMMA$_{20k}$-*b*-P*n*BA$_{135k}$-*b*-PMMA$_{20k}$, confirming the stability of the triblock copolymer architecture under these conditions.

The influence of the hard block composition on viscoelastic properties was further investigated through rheological measurements. Figure 7A displays the temperature dependence of G' for representative triblock copolymers having similar hard/soft block ratio.

https://doi.org/10.1021/acs.macromol.4c01233
Macromolecules 2024, 57, 9565−9575

Table 3. Experimental Conditions and Results of Triblock Copolymer Polymerizations[a]

entry	macro-CTA	[M]/[CTA]/[I]	triblock copolymers	time, h	conversion, %[b]	$M_{n(theor)}$, kg mol^{-1}[c]	$M_{n(SEC)}$, kg mol^{-1}[d]	$Đ$ (M_w/M_n)[d]
1	$PMMA_{40k}$ (entry 7, T1)	900/1/0.1	$PMMA_{20k}$-*b*-P*n*BA_{135k}-*b*-$PMMA_{20k}$	20	86.6	139	174	1.05
2	$PMMA_{112k}$ (entry 8, T1)	15 000/1/0.3	$PMMA_{56k}$-*b*-P*n*$BA_{1.9M}$-*b*-$PMMA_{56k}$	30	63.9	1291	1980	1.43
3	$PiBoMA_{46k}$ (entry 13, T1)	1000/1/0.1	$PiBoMA_{23k}$-*b*-P*n*BA_{117k}-*b*-$PiBoMA_{23k}$	17	87.0	149	163	1.02
4	$PiBoMA_{46k}$ (entry 13, T1)	2500/1/0.1	$PiBoMA_{23k}$-*b*-P*n*BA_{285k}-*b*-$PiBoMA_{23k}$	42	68.4	269	331	1.09
5	P(*i*BoMA-*co*-MMA)$_{42k}$ (entry 19, T1)	900/1/0.1	P(*i*BoMA-*co*-MMA)$_{21k}$-*b*-P*n*BA_{99k}-*b*-P(*i*BoMA-*co*-MMA)$_{21k}$	40	75.6	144	141	1.05
6	$PiBoMA_{46k}$ (entry 13, T1)	1600/1/0.1	$PiBoMA_{23k}$-*b*-$PTHFA_{94k}$-*b*-$PiBoMA_{23k}$	2	14.7	79.8	66.1	1.31

[a]Reaction conditions: macro-CTA, I = AIBN (entry 1−5), V-70 (entry 6), Temperature = 60 °C (entry 1−5), 30 °C (entry 6), bulk conditions. [b]Determined by ^{1}H NMR. [c]Determined by the following equation: $M_{n(theor)}=(m_{(mon.)} \times conv._{(mon.)} \times M_{(RAFT\ agent)}/m_{(RAFT\ agent)})+M_{(RAFT\ agent)}$. [d]Determined by SEC-RI-MALS in THF.

As previously reported,[33] the PMMA-based triblock copolymer ($PMMA_{20k}$-*b*-P*n*BA_{135k}-*b*-$PMMA_{20k}$) behaves as a typical TPE material with storage modulus values in the order of 10^{5-6} Pa below the glass transition of the PMMA hard block (Figure 7A, black curve). Yet, this decrease is progressive and suggests a well-defined phase separation of hard and soft domains above the glass transition of PMMA. No order−disorder transition inherent to the mixing of the two phases is observed over the range of temperature investigated. This characteristic imparts excellent mechanical integrity to this particular triblock copolymer over a broad temperature range. Nevertheless, this feature could also limit the further development of this material, especially concerning its implementation in industrial processing techniques such as injection molding or extrusion, where low viscosity at high temperatures is a prerequisite. One solution to overcome this limitation would consist in decreasing the molar mass of the triblock copolymers, as T_{ODT} decreases with polymer chain length for constant block chemistry and given composition.[56,57]

The statistical introduction of bulky groups such as isobornyl in the hard blocks (P(*i*BoMA-*co*-MMA)$_{21k}$-*b*-P*n*BA_{99k}-*b*-P(*i*BoMA-*co*-MMA)$_{21k}$) only slightly modifies the viscoelastic behavior of the triblock copolymers, with storage modulus values of the same order as $PMMA_{20k}$-*b*-P*n*BA_{135k}-*b*-$PMMA_{20k}$ and no order−disorder transition (Figure 7A, red curve). In contrast, when *i*BoMA is used as a unique constituent of the hard phase ($PiBoMA_{23k}$-*b*-P*n*BA_{117k}-*b*-$PiBoMA_{23k}$), the decrease of G' with increasing temperature is steeper (Figure 7A, blue curve), which hints at a lower segregation strength of the system under study. Indeed, a sudden drop of G' is observed after 200 °C, suggesting a probable order−disorder transition of the segregated structure.

Further investigation of the segregation behavior of these triblock copolymers was pursued by SAXS. Figure 7B shows the SAXS profiles obtained at 150 °C for a series of TPE materials with similar compositions and different hard blocks. As attested by the SAXS profiles, all samples are segregated at 150 °C, confirming the phase separation of the systems in both hard and soft domains (similar results (Figure S19) were obtained at 25 °C, with no hints of order−order transitions over this temperature span). A sequence of peaks at scattering wavevectors, indexed as $q/q^* = 1, \sqrt{3}, \sqrt{4}, \sqrt{7}$, is clearly visible for $PMMA_{20k}$-*b*-P*n*BA_{135k}-*b*-$PMMA_{20k}$, which is consistent with a cylindrical mesostructure (lattice parameter, p = 37.9 nm). The SAXS profiles of P(*i*BoMA-*co*-MMA)$_{21k}$-*b*-P*n*BA_{99k}-*b*-P(*i*BoMA-*co*-MMA)$_{21k}$ (p = 30.1 nm) and $PiBoMA_{23k}$-*b*-P*n*BA_{117k}-*b*-$PiBoMA_{23k}$ (p = 40 nm) samples only display a first order peak, and thus, it is difficult to assign a morphology without ambiguity.

CONCLUSIONS

The symmetrical TTC **TTC-bCP** was used to synthesize different high molar mass (M_n > 150 kg mol^{-1}) all-(meth)acrylic triblock copolymers exhibiting remarkably low dispersities ($Đ$ < 1.10) by RAFT polymerization. Through a convergent two-step process and using MMA and *i*BoMA monomers either alone or in mixtures of various proportions, it was possible to tune the glass transition temperature of the hard domains between 120 and 180 °C. Then, the successful synthesis of the soft acrylate midblock allowed the synthesis of hard−soft−hard triblock copolymers of controlled molar mass and composition. The thermal stability of the TTC midchain

https://doi.org/10.1021/acs.macromol.4c01233
Macromolecules 2024, 57, 9565−9575

Table 4. Thermal Properties of the Hard Block and Triblock Copolymers[a]

entry	polymer	$T_{g(\text{hard block})}$, °C	$T_{g(\text{soft block})}$, °C
1	PMMA	121	
2	P(*i*BoMA-*co*-MMA) (50/50)	131	
3	P(*i*BoMA-*co*-MMA) (75/25)	155	
4	P*i*BoMA	181	
5	PMMA-*b*-P*n*BA-*b*-PMMA	124	−57
6	P*i*BoMA-*b*-P*n*BA-*b*-P*i*BoMA	n.o.	−52
7	P(*i*BoMA-*co*-MMA)-*b*-P*n*BA-*b*-P(*i*BoMA-*co*-MMA) (*i*BoMA/MMA = 50/50)	n.o.	−60
8	P(*i*BoMA-*co*-MMA)-*b*-P*n*BA-*b*-P(*i*BoMA-*co*-MMA) (*i*BoMA/MMA = 75/25)	157	−48
9	P*i*BoMA-*b*-PTHFA-*b*-P*i*BoMA	172	−9

[a]n.o.: not observable. Entry 1 taken from ref 33.

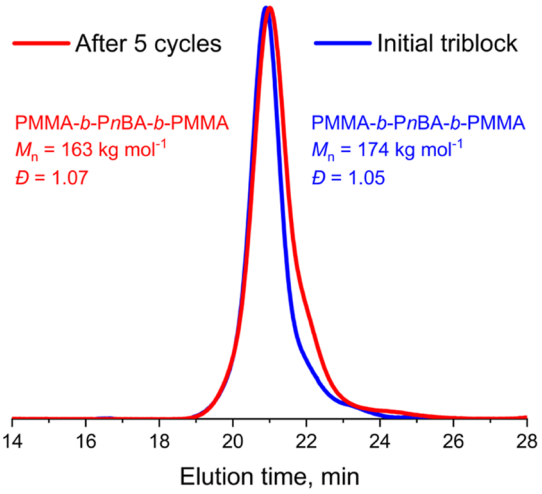

Figure 6. SEC-RI chromatograms of $PMMA_{20k}$-*b*-P*n*BA_{135k}-*b*-$PMMA_{20k}$ before and after exposure of 180 °C for 30 min (5 times).

group in copolymers was verified by SEC analyses and after material exposure to 180 °C (5 cycles) without loss of TPE properties, demonstrating the integrity of the macromolecular triblock architecture. Both viscoelastic and scattering data concluded on the phase separation into hard and soft domains of these systems, with, in particular, accessible order−disorder transition for the triblock system based on pure P*i*BoMA hard blocks. This clearly demonstrates the interest in fine structural design of the hard blocks in order to tune the final viscoelastic and mechanical properties of this new class of TPEs.

■ ASSOCIATED CONTENT

Supporting Information

The Supporting Information is available free of charge at https://pubs.acs.org/doi/10.1021/acs.macromol.4c01233.

NMR spectra of studied compounds; additional SEC chromatograms; and thermal analysis of the polymers (PDF)

■ AUTHOR INFORMATION

Corresponding Authors

Marc Guerre − *Laboratoire SOFTMAT, CNRS UMR 5623, Université of Toulouse, Université Toulouse III-Paul Sabatier, F-31062 Toulouse, France;* orcid.org/0000-0003-1410-9923; Email: marc.guerre@cnrs.fr

Mathias Destarac − *Laboratoire SOFTMAT, CNRS UMR 5623, Université of Toulouse, Université Toulouse III-Paul Sabatier, F-31062 Toulouse, France;* orcid.org/0000-0002-9718-2239; Email: mathias.destarac@univ-tlse3.fr

Authors

Maksym Odnoroh − *Laboratoire SOFTMAT, CNRS UMR 5623, Université of Toulouse, Université Toulouse III-Paul Sabatier, F-31062 Toulouse, France;* orcid.org/0000-0001-9177-5730

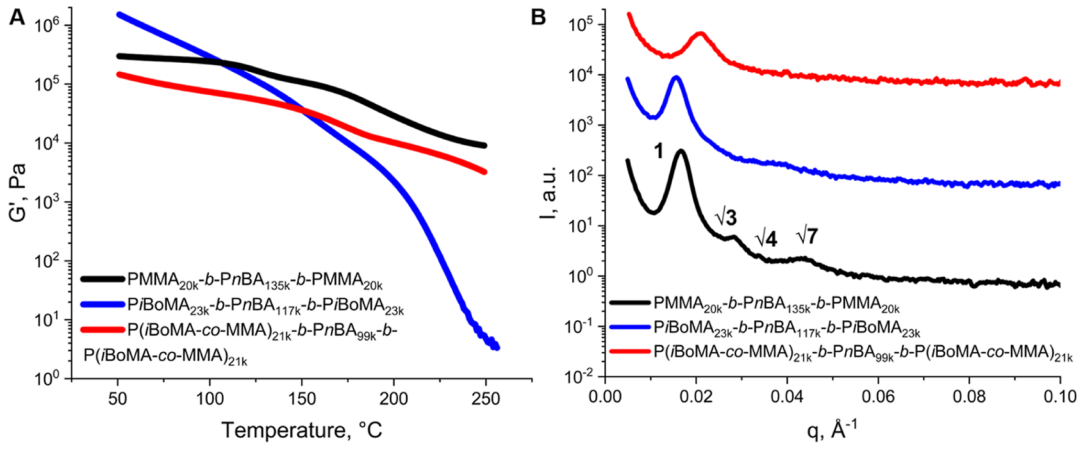

Figure 7. (A) Isochronal temperature ramp tests upon heating at 2.5 °C/min for $PMMA_{20k}$-*b*-P*n*BA_{135k}-*b*-$PMMA_{20k}$, P*i*$BoMA_{21k}$-*b*-P*n*BA_{117k}-*b*-P*i*$BoMA_{23k}$ and P(*i*BoMA-*co*-MMA)$_{21k}$-*b*-P*n*BA_{99k}-*b*-P(*i*BoMA-*co*-MMA)$_{21k}$ triblock copolymers. (B) SAXS spectra of $PMMA_{20k}$-*b*-P*n*BA_{135k}-*b*-$PMMA_{20k}$, P*i*$BoMA_{23k}$-*b*-P*n*BA_{117k}-*b*-P*i*$BoMA_{23k}$, and P(*i*BoMA-*co*-MMA)$_{21k}$-*b*-P*n*BA_{99k}-*b*-P(*i*BoMA-*co*-MMA)$_{21k}$ triblock copolymers acquired at 150 °C. Data have been shifted vertically for clarity.

https://doi.org/10.1021/acs.macromol.4c01233
Macromolecules 2024, 57, 9565−9575

Oleksandr Ivanchenko − *Laboratoire SOFTMAT, CNRS UMR 5623, Université of Toulouse, Université Toulouse III-Paul Sabatier, F-31062 Toulouse, France;* orcid.org/0000-0002-6006-7165

Guillaume Fleury − *Université de Bordeaux, CNRS, Bordeaux INP, LCPO, UMR 5629, F-33600 Pessac, France*

Complete contact information is available at: https://pubs.acs.org/10.1021/acs.macromol.4c01233

Notes

The authors declare no competing financial interest.

■ ACKNOWLEDGMENTS

The authors thank Pascale Laborie, Institut de Chimie de Toulouse ICT-UAR 599, and Lucie Perquis, Assistante Ingénieur CNRS, for their valuable respective help with SEC and DSC analyses.

■ REFERENCES

(1) Cheremisinoff, N. P. In *Condensed Encyclopedia of Polymer Engineering Terms*; Butterworth-Heinemann: Boston, 2001; pp 301−326. DOI: .

(2) Drobny, J. G. 2—Brief History of Thermoplastic Elastomers. In *Handbook of Thermoplastic Elastomers*, 2 ed.; Drobny, J. G., Ed.; *Plastics Design Library*; William Andrew Publishing: Oxford, 2014; pp 13−15..

(3) Gregory, G. L.; Sulley, G. S.; Kimpel, J.; Łagodzińska, M.; Häfele, L.; Carrodeguas, L. P.; Williams, C. K. Block Poly(Carbonate-Ester) Ionomers as High-Performance and Recyclable Thermoplastic Elastomers. *Angew. Chem., Int. Ed.* **2022**, *61* (47), No. e202210748.

(4) Wang, W.; Lu, W.; Goodwin, A.; Wang, H.; Yin, P.; Kang, N.-G.; Hong, K.; Mays, J. W. Recent Advances in Thermoplastic Elastomers from Living Polymerizations: Macromolecular Architectures and Supramolecular Chemistry. *Prog. Polym. Sci.* **2019**, *95*, 1−31.

(5) Woern, A. L.; Pearce, J. M. Distributed Manufacturing of Flexible Products: Technical Feasibility and Economic Viability. *Technologies* **2017**, *5* (4), 71.

(6) Bhowmick, A. K., Howard, S.. *Handbook of Elastomers*, 2nd ed.; CRC Press: Boca Raton, 2014..

(7) Fakirov, S. *Handbook of Condensation Thermoplastic Elastomers*; Wiley, 2005.

(8) Holden, G. *Thermoplastic Elastomers*, 2nd ed.; Hanser Publishers: Munich, 1996.

(9) Hsieh, H.; Quirk, R. P. Styrenic Thermoplastic Elastomers. In *Anionic Polymerization*; CRC Press, 1996.

(10) Hsieh, H.; Quirk, R. P. Applications of Styrenic Thermoplastic Rubbers in Plastics Modifications, Adhesives, and Footwears. In *Anionic Polymerization*; CRC Press, 1996.

(11) Wang, B.; Long, Y.-Y.; Li, Y.-G.; Men, Y.-F.; Li, Y.-S. Cyclic Olefin Copolymers of Propylene with Asymmetric Si-Containing α,ω-Diolefins: The Tailored Thermal and Mechanical Properties. *Polymer* **2015**, *61*, 108−114.

(12) Jiang, F.; Wang, Z.; Qiao, Y.; Wang, Z.; Tang, C. A Novel Architecture toward Third-Generation Thermoplastic Elastomers by a Grafting Strategy. *Macromolecules* **2013**, *46* (12), 4772−4780.

(13) Dufour, B.; Tang, C.; Koynov, K.; Zhang, Y.; Pakula, T.; Matyjaszewski, K. Polar Three-Arm Star Block Copolymer Thermoplastic Elastomers Based on Polyacrylonitrile. *Macromolecules* **2008**, *41* (7), 2451−2458.

(14) Bolton, J. M.; Hillmyer, M. A.; Hoye, T. R. Sustainable Thermoplastic Elastomers from Terpene-Derived Monomers. *ACS Macro Lett.* **2014**, *3* (8), 717−720.

(15) Maji, P.; Naskar, K. Styrenic Block Copolymer-Based Thermoplastic Elastomers in Smart Applications: Advances in Synthesis, Microstructure, and Structure−Property Relationships—A Review. *J. Appl. Polym. Sci.* **2022**, *139* (39), No. e52942.

(16) Kang, B.-G.; Shoji, H.; Kataoka, H.; Kurashima, R.; Lee, J.-S.; Ishizone, T. Living Anionic Polymerization of N-(1-Adamantyl)-N-4-Vinylbenzylideneamine and N-(2-Adamantyl)-N-4-Vinylbenzylideneamine: Effects of Adamantyl Groups on Polymerization Behaviors and Thermal Properties. *Macromolecules* **2015**, *48* (23), 8489−8496.

(17) Matsuoka, D.; Goseki, R.; Uchida, S.; Ishizone, T. Living Anionic Polymerization of 1-Adamantyl 4-Vinylphenyl Ketone. *Macromol. Chem. Phys.* **2017**, *218* (12), 1700015.

(18) Kobayashi, S.; Kataoka, H.; Goseki, R.; Ishizone, T. Living Anionic Polymerization of 4-(1-Adamantyl)-α-Methylstyrene. *Macromol. Chem. Phys.* **2018**, *219* (1), 1700450.

(19) Hutchings, L. R.; Brooks, P. P.; Shaw, P.; Ross-Gardner, P. Fire and Forget! One-Shot Synthesis and Characterization of Block-Like Statistical Terpolymers via Living Anionic Polymerization. *J. Polym. Sci., Part A: Polym. Chem.* **2019**, *57* (3), 382−394.

(20) Hutchings, L. R.; Brooks, P. P.; Parker, D.; Mosely, J. A.; Sevinc, S. Monomer Sequence Control via Living Anionic Copolymerization: Synthesis of Alternating, Statistical, and Telechelic Copolymers and Sequence Analysis by MALDI ToF Mass Spectrometry. *Macromolecules* **2015**, *48* (3), 610−628.

(21) Chen, J.-K.; Kuo, S.-W.; Kao, H.-C.; Chang, F.-C. Thermal Properties, Specific Interactions, and Surface Energies of PMMA Terpolymers Having High Glass Transition Temperatures and Low Moisture Absorptions. *Polymer* **2005**, *46* (7), 2354−2364.

(22) Gunaydin, A.; Mugemana, C.; Grysan, P.; Eloy Federico, C.; Dieden, R.; Schmidt, D. F.; Westermann, S.; Weydert, M.; Shaplov, A. S. Reinforcement of Styrene Butadiene Rubber Employing Poly(Isobornyl Methacrylate) (PIBOMA) as High Tg Thermoplastic Polymer. *Polymers* **2021**, *13* (10), 1626.

(23) Nakano, Y.; Sato, E.; Matsumoto, A. Synthesis and Thermal, Optical, and Mechanical Properties of Sequence-Controlled Poly(1-Adamantyl Acrylate)-Block-Poly(n-Butyl Acrylate) Containing Polar Side Group. *J. Polym. Sci., Part A: Polym. Chem.* **2014**, *52* (20), 2899−2910.

(24) Ding, W.; Wang, S.; Yao, K.; Ganewatta, M. S.; Tang, C.; Robertson, M. L. Physical Behavior of Triblock Copolymer Thermoplastic Elastomers Containing Sustainable Rosin-Derived Polymethacrylate End Blocks. *ACS Sustainable Chem. Eng.* **2017**, *5* (12), 11470−11480.

(25) Hamada, K.; Morishita, Y.; Kurihara, T.; Ishiura, K. Methacrylate-Based Polymers for Industrial Uses. In *Anionic Polymerization: Principles, Practice, Strength, Consequences and Applications*; Hadjichristidis, N., Hirao, A., Eds.; Springer Japan: Tokyo, 2015; pp 1011−1031..

(26) Self-Assembling Acrylic Block Copolymers for Enhanced Adhesives Properties; Adhesives Magazine Adhesives & Sealants Industry, 2013−05−01. https://www.adhesivesmag.com/articles/91909-self-assembling-acrylic-block-copolymers-for-enhanced-adhesives-properties (accessed 11-23, 2023).

(27) Tong, J. D.; Moineau, G.; Leclère, P.; Brédas; Lazzaroni, R.; Jérôme, R. Synthesis, Morphology, and Mechanical Properties of Poly(Methyl Methacrylate)-b-Poly(n-Butyl Acrylate)-b-Poly(Methyl Methacrylate) Triblocks. Ligated Anionic Polymerization vs Atom Transfer Radical Polymerization. *Macromolecules* **2000**, *33* (2), 470−479.

(28) Lu, W.; Wang, Y.; Wang, W.; Cheng, S.; Zhu, J.; Xu, Y.; Hong, K.; Kang, N.-G.; Mays, J. All Acrylic-Based Thermoplastic Elastomers with High Upper Service Temperature and Superior Mechanical Properties. *Polym. Chem.* **2017**, *8* (37), 5741−5748.

(29) Atkinson, R. L.; Monaghan, O. R.; Elsmore, M. T.; Topham, P. D.; Toolan, D. T. W.; Derry, M. J.; Taresco, V.; Stockman, R. A.; De Focatiis, D. S. A.; Irvine, D. J.; Howdle, S. M. RAFT Polymerisation of Renewable Terpene (Meth)Acrylates and the Convergent Synthesis of Methacrylate−Acrylate−Methacrylate Triblock Copolymers. *Polym. Chem.* **2021**, *12* (21), 3177−3189.

(30) Chernikova, E. V.; Terpugova, P. S.; Baskakov, A. A.; Plutalova, A. V.; Garina, E. S.; Sivtsov, E. V. Pseudoliving Radical Polymerization of Methyl Methacrylate in the Presence of S,S′-Bis(Methyl-2-

Isobutyrate) Trithiocarbonate. *Polym. Sci., Ser. B* **2010**, *52* (3−4), 119−128.
(31) Lai, J. T.; Filla, D.; Shea, R. Functional Polymers from Novel Carboxyl-Terminated Trithiocarbonates as Highly Efficient RAFT Agents. *Macromolecules* **2002**, *35* (18), 6754−6756.
(32) Ma, J.; Zhang, H. Kinetic Investigations of RAFT Polymerization: Difunctional RAFT Agent Mediated Polymerization of Methyl Methacrylate and Styrene. *Macromol. Res.* **2015**, *23* (1), 67−73.
(33) Ivanchenko, O.; Odnoroh, M.; Mallet-Ladeira, S.; Guerre, M.; Mazières, S.; Destarac, M. Azo-Derived Symmetrical Trithiocarbonate for Unprecedented RAFT Control. *J. Am. Chem. Soc.* **2021**, *143* (49), 20585−20590.
(34) Agilent Polymer Standards for GPC/SEC. https://www.agilent.com/cs/library/usermanuals/public/5991-7911EN.pdf Accessed on May 15, 2024.
(35) Malihi, F. B.; Kuo, C.-Y.; Provder, T. Determination of the Absolute Molecular Weight of a Styrene−Butyl Acrylate Emulsion Copolymer by Low-Angle Laser Light Scattering (LALLS) and GPC/LALLS. *J. Appl. Polym. Sci.* **1984**, *29* (3), 925−931.
(36) Zhang, X. Q.; Wang, C. H. Solution Characterization of Poly(Isobornyl Methacrylate) in Tetrahydrofuran. *J. Polym. Sci., Part B: Polym. Phys.* **1994**, *32* (11), 1951−1956.
(37) Zioga, A.; Ekizoglou, N.; Siakali-Kioulafa, E.; Hadjichristidis, N. Characteristic Ratio of Poly(Tetrahydrofurfuryl Acrylate) and Poly(2-Ethylbutyl Acrylate). *J. Polym. Sci., Part B: Polym. Phys.* **1997**, *35* (10), 1589−1592.
(38) Hajiali, F.; Tajbakhsh, S.; Marić, M. Thermal Characteristics and Flame Retardance Behavior of Phosphoric Acid-Containing Poly(Methacrylates) Synthesized by RAFT Polymerization. *Mater. Today Commun.* **2020**, *25*, 101618.
(39) Rajendrakumar, K.; Dhamodharan, R. Spontaneous Cu(I)Br−PMDETA-Mediated Polymerization of Isobornyl Methacrylate in Heterogeneous Aqueous Medium at Ambient Temperature. *J. Polym. Sci., Part A: Polym. Chem.* **2011**, *49* (10), 2165−2172.
(40) Beuermann, S.; Buback, M.; Davis, T. P.; Gilbert, R. G.; Hutchinson, R. A.; Olaj, O. F.; Russell, G. T.; Schweer, J.; van Herk, A. M. Critically Evaluated Rate Coefficients for Free-Radical Polymerization, 2. Propagation Rate Coefficients for Methyl Methacrylate. *Macromol. Chem. Phys.* **1997**, *198* (5), 1545−1560.
(41) Beuermann, S.; Buback, M.; Davis, T. P.; García, N.; Gilbert, R. G.; Hutchinson, R. A.; Kajiwara, A.; Kamachi, M.; Lacík, I.; Russell, G. T. Critically Evaluated Rate Coefficients for Free-Radical Polymerization, 4. *Macromol. Chem. Phys.* **2003**, *204* (10), 1338−1350.
(42) Brostow, W.; Chiu, R.; Kalogeras, I. M.; Vassilikou-Dova, A. Prediction of Glass Transition Temperatures: Binary Blends and Copolymers. *Mater. Lett.* **2008**, *62* (17−18), 3152−3155.
(43) Yeh, S.-L.; Zhu, C.-Y.; Kuo, S.-W. Transparent Heat-Resistant PMMA Copolymers for Packing Light-Emitting Diode Materials. *Polymers* **2015**, *7* (8), 1379−1388.
(44) Park, S. I.; Lee, S. I.; Hong, S.-J.; Cho, K. Y. Suspension Polymerization and Characterization of Transparent Poly(Methyl Methacrylate-Co-Isobornyl Methacrylate). *Macromol. Res.* **2007**, *15* (5), 418−423.
(45) Tong, J. D.; Jerôme, R. Synthesis of Poly(Methyl Methacrylate)-b-Poly(n-Butyl Acrylate)-b-Poly(Methyl Methacrylate) Triblocks and Their Potential as Thermoplastic Elastomers. *Polymer* **2000**, *41* (7), 2499−2510.
(46) Tong, J.-D.; Jerôme, R. Dependence of the Ultimate Tensile Strength of Thermoplastic Elastomers of the Triblock Type on the Molecular Weight between Chain Entanglements of the Central Block. *Macromolecules* **2000**, *33* (5), 1479−1481.
(47) Carmean, R. N.; Becker, T. E.; Sims, M. B.; Sumerlin, B. S. Ultra-High Molecular Weights via Aqueous Reversible-Deactivation Radical Polymerization. *Chem* **2017**, *2* (1), 93−101.
(48) Yan, K.; Gao, X.; Luo, Y. Well-Defined High Molecular Weight Polystyrene with High Rates and High Livingness Synthesized via Two-Stage RAFT Emulsion Polymerization. *Macromol. Rapid Commun.* **2015**, *36* (13), 1277−1282.
(49) Truong, N. P.; Dussert, M. V.; Whittaker, M. R.; Quinn, J. F.; Davis, T. P. Rapid Synthesis of Ultrahigh Molecular Weight and Low Polydispersity Polystyrene Diblock Copolymers by RAFT-Mediated Emulsion Polymerization. *Polym. Chem.* **2015**, *6* (20), 3865−3874.
(50) Read, E.; Guinaudeau, A.; James Wilson, D.; Cadix, A.; Violleau, F.; Destarac, M. Low Temperature RAFT/MADIX Gel Polymerisation: Access to Controlled Ultra-High Molar Mass Polyacrylamides. *Polym. Chem.* **2014**, *5* (7), 2202−2207.
(51) Rzayev, J.; Penelle, J. HP-RAFT: A Free-Radical Polymerization Technique for Obtaining Living Polymers of Ultrahigh Molecular Weights. *Angew. Chem., Int. Ed.* **2004**, *43* (13), 1691−1694.
(52) Haloi, D. J.; Ata, S.; Singha, N. K.; Jehnichen, D.; Voit, B. Acrylic AB and ABA Block Copolymers Based on Poly(2-Ethylhexyl Acrylate) (PEHA) and Poly(Methyl Methacrylate) (PMMA) via ATRP. *ACS Appl. Mater. Interfaces* **2012**, *4* (8), 4200−4207.
(53) Bekanova, M. Z.; Neumolotov, N. K.; Jablanović, A. D.; Plutalova, A. V.; Chernikova, E. V.; Kudryavtsev, Y. V. Thermal Stability of RAFT-Based Poly(Methyl Methacrylate): A Kinetic Study of the Dithiobenzoate and Trithiocarbonate End-Group Effect. *Polym. Degrad. Stab.* **2019**, *164*, 18−27.
(54) KURARITY. *Acrylic Block Copolymer Technical Information*.
(55) Hornung, C. H.; Postma, A.; Saubern, S.; Chiefari, J. Sequential Flow Process for the Controlled Polymerisation and Thermolysis of RAFT-Synthesised Polymers. *Polymer* **2014**, *55* (6), 1427−1435.
(56) Leibler, L. Theory of Microphase Separation in Block Copolymers. *Macromolecules* **1980**, *13* (6), 1602−1617.
(57) Matsen, M. W.; Schick, M. Stable and Unstable Phases of a Diblock Copolymer Melt. *Phys. Rev. Lett.* **1994**, *72* (16), 2660−2663.

https://doi.org/10.1021/acs.macromol.4c01233
Macromolecules 2024, 57, 9565−9575